Journal of Nanomedicine & Nanotechnology
ISSN: 2157-7439
OPEN ACCESS Freely available online
Image Article

On Non-Invasive Measurements of Exhaled Aceton Using Metal Oxide Nanosensors

Aroutiounian VM*

Yerevan State University, Yerevan, Armenia

ABSTRACT

The paper presents and discusses works carried out both at Yerevan State University and abroad on non-invasive metal oxide sensors (chemiresistors) for acetone exhaled by a diabetic. The technologies and parameters of chemiresistors based on tin dioxide, tungsten trioxide, zinc oxide, Fe_2O_3, In_2O_3 and TiO_2 developed at YSU and in the world are presented. Most likely, it makes sense to start investigations start with concentration 1 ppm acetone. The response of the MWCNT-doped SnO_2 chemiresistors was measured at a concentration of acetone from 1 to 12 ppm, characteristic of diabetics at a relatively early stage of the disease.

Keywords: Human breath; Biomarkers

INTRODUCTION

Human breath is a complicated mixture of different gases including carbon dioxide, water vapor, oxygen, nitrogen, and trace levels of more than 1000 compounds which are either generated in the body (endogenous) or absorbed from the environment (exogenous) [1]. Human breath has been used as a potential tool for the diagnosis and study of diseases [2,3].The presence of biomarkers in the exhaled breath is suggestive for a number of medical conditions, such as lung cancer [4,5], breast cancer [6], asthma andchronic obstructivepulmonary disease (COPD) [7], and diabetes [8,9]. A few volatile organic compounds (VOCs) have been regarded as biomarkers to diagnose diseases, for example, formaldehyde and toluene (lung cancer), ammonia (hemodialysis), H2S (halitosis), isoprene (heart disease), benzene (smoker), and pentane (acute asthma) are known as biomarkers for patients.

Recently, scientists have grown interested in solid-state sensors [10-19] for detecting VOCs for non-invasive diabetes management. According to the World Health Organization, currently there are around 450 million peoples suffering from diabetes in the world, and this number could potentially reach 700 million by 2045. The number of patients with diabetes mellitus in Armenia today is 73 thousand.

As was mentioned above, human exhaled breath contains thousands of different volatile organic compounds (VOCs) derived from the body's metabolic processes. In patients with diabetes mellitus, the body produces excess amounts of ketones [20] such as acetone because the body uses fats instead of glucose to produce energy, which is then exhaled during respiration. Endogenous acetone is produced in the liver primarily through ketogenesis. In certain cases, such as fasting, exercising and being diabetic, the liver produces ketones to act as an additional energy source, which is then metabolized into acetone and other ketone bodies. Using breath analysis techniques, acetone concentrations in the exhaled breath have been shown to correlate with the acetone concentrations in the blood as well as with other ketones such as beta-hydroxybutyrate.

Measurement of breath acetone may provide better diagnostic control of a patient's diabetic condition than using blood glucose alone [21]. At the same time, the detection of the concentration of acetone in the exhaled air can be carried out in a quick and acceptable way for the patient, alternative to the traditional methods for determining glucose in the blood. Many diabetic patients today have to check their blood sugar several times a day, which requires frequent and repeated pricking of their fingers, which is painful and unsafe. It has been established that glucose is also detected in the analysis of tears, saliva, and urine, but their corresponding meters at the commercial level are not yet available to patients.

So, acetone is considered today as the main breath biomarker for metabolic (diabetes) conditions in the bloodstream. It is found that the acetone concentration in exhaled breath of healthy people is ranged between 0.3 and 1. 0. ppm. Diabetes is one of the factors that may cause a change in breath acetone levels. Age, lifestyle, profession, and consuming ketogenic diet influenced breath acetone concentration and increase its concentration. Patients with typical symptoms of diabetes (polyuria, polydipsia and

***Correspondence to**: Aroutiounian VM, Yerevan State University, Yerevan, Armenia, E-mail:kisahar@ysu.am, aroutiounv1@yahoo.com

Received: February 16, 2021; **Accepted**: March 18, 2021; **Published:** March 25, 2021

Citation: Aroutiounian VM (2021) On Non-Invasive Measurements of Exhaled Aceton Using Metal Oxide Nanosensors. J Nanomed Nanotech. 12: 560.

unexplained weight loss) have a high blood glucose concentration. Apart from hyperglycemia, hypoglycemia would damage the human body as well. Clinically, hypoglycemiais determined as a condition where the blood glucose concentration is lower. For elderly patients, the risk coefficient of hypoglycemia is higher. The incidence ofhypoglycemia at night is relatively high, and it is difficult to monitor it with traditional blood glucose detection methods. Strict blood glucose control is also likely to increase the risk of hypoglycemia. Therefore, continuous glucose monitoring in diabetics may be of more clinical application value and more in line with market trends [1,22].

Measurement of the concentration of acetone in breath is necessary. Techniques such as gas chromatography coupled to mass spectrometry, solid-phase microextraction, high-performance liquid chromatography, selected ion flow tube mass spectrometry, and liquid chromatography-mass spectrometry [4] for the detection of different gases. Sensors can be easy prepared by several who have provided a highly selective analysis of VOCs in the breath. Although mentioned above analytical methods are very sensitive and selective for diagnosis of diabetes mellitus, they are expensive, non-portable, and cannot be used out of hospitals.

Chemiresistors made from metal oxides

Metal oxide semiconductor gas sensors widely used today modern microelectronic technology methods, have low cost and high sensitivity [10-19]. Further research in this field is carried out in direction of the dramatica decrease of operating temperature from 300-500^{0}C up to near-room temperature, understanding the phenomena on the surface of detectors, sensing mechanisms, and improvement of its selectivity to the gas. As electrical resistance in semiconductor metal oxide dramatically changes in the presence of an oxidizing or reducing gases, it is necessary often use only metal oxide-based chemiresistors for many applications. Several factors, such as surface areas, particle size, crystal defects, porous structures, and stoichiometry greatly affect the performance of such sensors. In particular, chemical gas sensors using various semiconducting metal oxides such as SnO_2, WO_3, ZnO, Fe_2O_3, and TiO_2, have been applied for acetone detection. Doping with metal or metal oxide and adding catalysts, particle size reducing, porosity and morphology controlling are used for the manufacturing of the most effective methods to improve gas sensing performance of the metal oxide semiconductor-based sensors. Some results of the best acetone detectors made of mentioned above semiconductors are discussed (see Table 1).

Chemiresistors made of tin dioxide

Tin dioxide SnO_2 with a wide band gap of 3.6 eV has been widely used to detect toxic chemicals such as CH_4, H_2, C_2H_5OH, gasoline, CO, C_2H_2, H_2O_2, NO_2, NO, NH_3, and H_2S. Pure (without impurities) SnO_2 and other metal oxide have low sensitivity to gases at its rather high pre-heating (operation) temperature. Doping of tin dioxide with some metals or carbon nanotubes is one way of improving the sensitivity of such metal oxide sensors. The sensitivity of SnO_2 sensors can be greatly improved by doping of the volume during a sensitizing of a material or dispersing on the oxide surface a low concentration of Co, Au, Pd, Pt, etc. For example, compared with sensors loaded with pure SnO_2 nanofibers, the Co-SnO_2 nanofiber sensors exhibited improved acetone sensing properties with high selectivity and rapid response and recovery times. Pure SnO_2nanofiber-based flat sensors have similar responses to acetone and ethanol. The Co-doped SnO_2 nanofiber-based flat sensors had more than five times larger response (sensitivity) than that of the sensors to ethanol. These results suggest that the addition of Co is beneficial to the selective acetone sensing properties of SnO_2nanofibers [6].

Acetone sensors made from SnO_2 doped with different impurities reported in [18,33]. A series of Co_3O_4-loaded tin dioxide nanocomposite thick films were prepared by grinding, screen printing and sintering in [34]. The composite films exhibited a good response to acetone at 300°C. At this temperature, the maximum sensor response to acetone (1000 ppm in the air) was 235, which was about 5 times as large as that of the pure SnO_2. The selectivity to acetone over H_2 and CO was also promoted by the addition of Co_3O_4 to SnO_2 [35]. Though Co_3O_4 is a p-type conductor and SnO_2 is a typical n-type conductor, the small mole rate of Co_3O_4 does not change it to a p-type. Measurements show an n-type response to reducing gases (the electrical resistance decreases on exposure to reducing gas) in air. The gas sensitivity exhibits a volcano-shaped relation with the operating temperature, reaching a maximum at 300◦C in each case. The addition of Co_3O_4 does not result in a shift of the volcano-shaped correlations between gas response and temperature toward the lower temperature side. This is different from Ag_2O- and PdO-loaded SnO_2 sensors which makes the best operating temperature shift toward the lower temperature side [36,37]. Note again that the response of 5 mol.% Co to alcohol and acetone is far larger than that of pure SnO_2, proving a very marked promoting effect of Co_3O_4 loading. The sensor response of pure Co_3O_4 to several gases (1000 ppm) at 300°C is quite small compared to the sensor response of pure SnO_2. The sensor response degrades

Table 1: Metal Oxides Based Acetone Sensors.

Sensor	Work Temp	Response (ppm)	Ref.
SnO_2<MWCNT>	250	4.70 <0.2> 1002<1000>	16,17, 23, 33
SnO_2<MWCNT>	200	120 <2.5>	24
SnO_2 NF <Graphene>	350	10.04 (5)	25
WO_3<Si>	400	1.5 (0,6)	26
WO_3<C>	300	3.6 (1)	27
WO_3<Pt>	300	2.67 (2)	28
WO_3<Cu>	300	2.88 (5)	29
WO_3<Graphene>	300	6.96(12)	30
WO_3 (RuO_2) Nanofiber	350	78.61 (5)	31
ZnO<Ce>	24	3 (5)	32

when excessive Co_3O_4 is added. Perhaps too many reactive sites make it more difficult for reducing gas molecules to disuse into the inner part of a thick film. At the optimal operating temperature of 180°C, the relationship between the sensitivity of the SnO_2 thick film and the acetone vapor concentration is shown in (Figure 2). The SnO_2 nanosensor is sensitive to low concentrations of acetone. T_A is the annealing temperature.

The mechanism of sensitivity to acetone and the properties of SnO_2 thick films are discussed in [38]. Acetone vapor sensing characteristics of cobalt-doped SnO_2 thin films were reported in [39]. Structural and microstructural studies of PbO-doped SnO_2 sensor for the detection of methanol, propanol, and acetone were carried out in [40]. Gas sensors based on samarium oxide loaded mulberry shaped tin oxide for highly selective and sub-ppm-level acetone detection were investigated in [41]. The response, selectivity, optimum operating temperature, response time, and recovery time were investigated in [42] for zinc, ceria, zinc with ceria doped and non-doped (pristine) SnO_2.

We discuss in [1,43] dimensional effects in small-size sensors. It was found also that the controlling particle size and porosity of the material can enhance the sensitivity of the material. Metal oxides with small grains, nanorods, nanotubes, nanowires, and so on can lead to the higher sensitivity of sensors made from them. The average grain size was reduced to several nanometers [1]. Tin oxide powders show higher sensor performance than corresponding metal oxide powder materials, which have a lower specific surface area. Microstructure plays a crucial role, and a sensor's sensitivity can be significantly increased by using materials with very small grain sizes. The response was 33 when the sensors were exposed to acetone at 330°C. The response and recovery times to acetone were

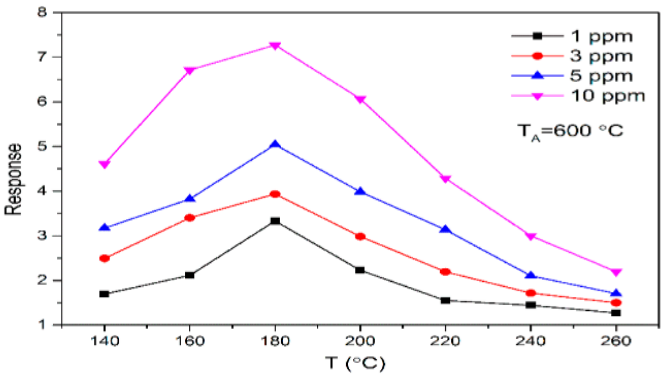

Figure 1: Response of sensors based on SnO2 nanoparticles versus operating temperature to 1, 3, 5, and 10 ppm acetone, respectively.

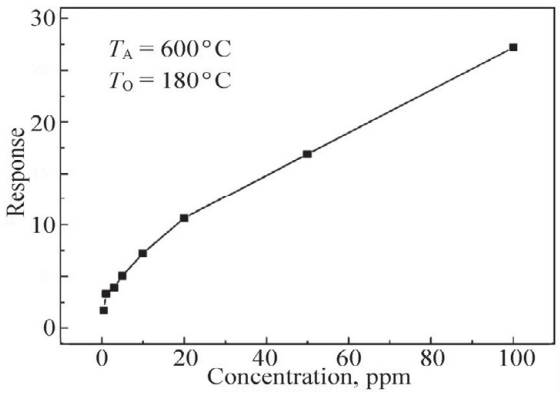

Figure 2: The response dependence on the acetone concentration for SnO_2 powders at the operating temperature of 180°C [18].

about 5 and 8 s, respectively [44].

For the detection of acetone, Choi et al. [45] used SnO_2 nanofilaments functionalized with reduced graphene oxide (RGO). A noticeable amount of acetone was achieved by increasing the RGO doping to 5 wt% and raising the operating temperature to 350° C. The predicted detection limit of acetone for these sensors at 5 wt% doping was only 100 bpm. Most likely, RGO formed continuous paths for the percolation of charged particles, which control electrical transport in nanofibers. The highly selective characteristics in the detection of acetone are apparently due to the combined synergistic effect of the porous nanotube morphology and the uniform distribution of Pt / PtO_x nanocatalysts on thin-walled SnO_2 nanotubes (NTs), which can provide both chemical and electronic sensitization. In addition, in [45], sensors were developed with three different sensitive layers (NT Pt-PS SnO_2, NT Pt- SnO_2, and NT PS- SnO_2 [46-49].

A heterostructure acetone sensor made from NiO-doped SnO_2 hollow nanofilaments with porous structures through the combination of electrospinning technique and calcination procedure was developed [50]. The excellent sensing performances of the proposed sensor were ascribed to its hollow-core structure and Ni doping. In fact, the presence of heterojunctions formed by the combination of p-type NiO and n-type SnO_2 increased the sensor resistance and sensory responses to acetone vapor. The enhanced acetone sensing can be ascribed to the formation of p-n junction between p-type NiO and n-type SnO_2 grains. The gas sensor based on NiO- SnO_2 nanofibers has a maximum gas response at the operating temperature of 275°C, while the sensor based on NiO shows the highest responses at 325°C. NiO-SnO_2 exhibits a better selectivity than NiO, having a preferential response to acetone. Therefore, the NiO- SnO_2 nanofibers could be used for selective acetone detection. Furthermore, the long-time stability of NiO and NiO- SnO_2 are also highly sensitive measured. Both sensors exhibit good stability towards 20 ppm acetone in 60 days. Acetone sensors based on SnO_2, doped with Eu are reported in [51,52]. Work temperature was 280°C for such sensors. Y-doped SnO_2 nanosensors were developed in [53].

Sensors made from metal oxides doped with carbon nanotubes (CNTs) have higher sensitivity and better stability of the sensor [8].

Acetone sensors made from SnO_2 <MWCNT>nanocomposites

It was shown in Yerevan State University [16] that the functionalized SnO_2 with multi-walled carbon nanotube (MWCNT) thick-film structures with Ru catalyzer leads to a considerable increase in response signal to the VOC gases. Structures were obtained by hydrothermal synthesis and sol-gel techniques as well as their combination. The choice of corresponding treating conditions and regimes for CNTs functionalization as well as thick film surface modification with Ru catalyst were focused in [16,54,55]. The testing of all samples at different operating temperatures in other to compare responses to various considered here target VOCs was carried out.

The largest and sufficiently selective response to acetone vapors (Ra/Rg = 1002) at their concentration of 1000 ppm is achieved at samples with 1:200 (MWCNT: SnO_2) mass ratio of the components. The largest response to acetone vapors (Ra/Rg = 555, 62) is fixed for such a set of samples to acetone vapors exposure 1000 ppm at 250°C operating temperature. Selective sensitivity of acetone vapors sensors with 1:50 mass ratio of the components

appears only at the 300°C operating temperature.

As an example, the dependence of the 1:200 sensor response vs acetone vapor concentration at 150°C is presented in Figure 3. Note that the gas response increases linearly with acetone vapor concentration in its large range. It opens a possibility to realize an easy detector/measurer of the concentration of acetone in the air or exhaled breath gas.

It is obvious today that the doping of metal oxide with CNTs leads to better sensitivity and lower preheating of the work body of a hybrid sensor. Note that several complicate phenomena processes take place in such functionalized nanocomposites. The full picture is not possible to propose today, but we have to take into account the following: MWCNTs have a huge specific surface area and a nanoscale structure, which exposes a large number of sites at which the gases can react. Detection of various gases can be provided at low temperatures of pre-heating of the work body of a sensor. The electric conductivity of CNTs is much higher in comparison with the conductivity of metal oxides. Therefore, CNTs reduce the resistance of the sensing metal oxide materials and open the possibility for the percolation of charge carriers through the sample. Since a metal oxide film has mainly n-type semiconductor characteristics and MWCNTs have p-type semiconductor characteristics, there are two

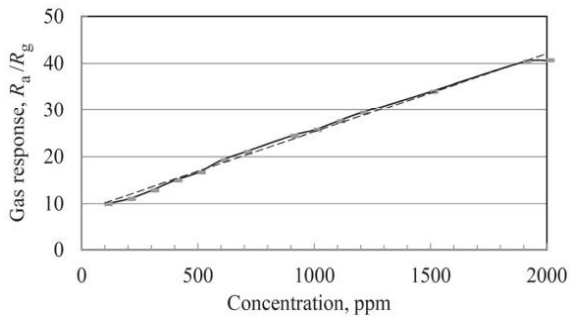

Figure 3: Dependence of the SnO_2<MWCNT> sensor response vs acetone vapor concentration.

depletion layers in such hybrid films. Note that the first depletion region is located at the metal oxide surface and the second one is located in the interface between the metal oxide nanoparticle and the MWCNTs. Formation of nanochannels and heterojunctions leads to enhanced gas sensitivity of such hybridized gas sensors as the decrease in the work function (barrier height) or increase in the conductivity of the metal oxide sensitive layer leads to the improvement in the performance of the gas sensor at low operating temperature.

The response of the prepared sensor toward 1 ppm acetone vapor at 250°C was presented in Figure 4. It is shown that the resistance decreases very sharply after exposure of acetone.

The addition of MWCNTs improves significantly the sensitivity of SnO_2. The sensitivity study was carried out for different concentrations of MWCNT to get the highest response as shown in Figure 4b. It is to be noted that the highest sensitivity was achieved for SnO_2 loaded in 0.25% MWCNTs. The over-addition of MWCNTs in the composite decreases the resistance of the sensor sharply. For over-addition of MWCNTs, the increasing number of electrons in the grain boundary reduce the resistance and increase the sensitivity of the sensors. The response toward acetone vapor was jumped to 72% after the addition of 0.25% MWCNT. The response of sensors made from pure nanocrystalline SnO_2 and SnO_2 loaded in 0.25% MWCNTs toward 1 ppm acetone for different operating temperatures is shown in Figure 4c. 0.25% MWCNT loaded SnO_2 sensor showed a much better response at the lower temperature. The sub-ppm level acetone sensing at 350°C is presented in Figure 4d.

Note that nanonsensors to hydrogen dioxide made of SnO_2<MWCNT> were reported also in [14,16,17] and ZnO<CNT>-in [56]. Ahmadnia-Feyzabad *et al.* [57] also fabricated multiwall carbon nanotubes 1:200 MWCNT/ SnO_2 sensors using the ultrasonic-assisted deposition-precipitation method and they were used for detection of four VOCs, including acetone.

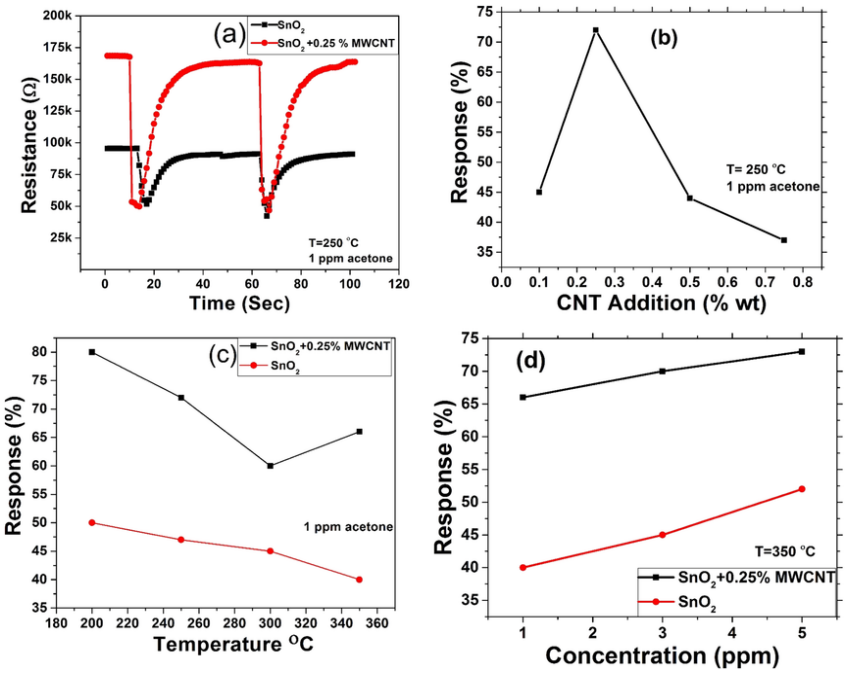

Figure 4(a) The response of SnO_2 and SnO_2<0.25% MWCNT> sensors in 1 ppm acetone at 250°C.
(b) The response of SnO_2 sensor in 1 ppm acetone for different CNT loadings at 250°C.
(c) The response of SnO_2 and SnO_2<0.25% MWCNT>nanocomposite sensors in 1 ppm acetone at different temperatures.
(d) The response of SnO2 and SnO_2<0.25% MWCNT> sensors in different concentrations of acetone at 350°C.

Significant enhancement of the sensor selectivity to acetone with respect to gases like toluene and trichloroethylene was observed. Narjinaryet *al.* [57] developed highly sensitive and stable acetone sensor by using MWCNTs as a substrate for sol-gel prepared nanocrystalline SnO_2. It was mentioned that the enhancement in sensing performance was due to the formation of hetero-junction and an increase in adsorptioncapacity because of the higher surface area of MWCNT.

WO3 Based Chemiresistors

N-type tungsten trioxide (WO_3) with a bandgap of 2.6 eV is known as a promising material for VOCs sensing. Although most of the reported WO_3 gas sensors are based on its *gamma-* phase [58], *epsilon-* WO_3 is used for selective and sensitive detection of acetone in ppb concentrations which is attributed to the spontaneous electric dipole moment of the *epsilon*–phase that increases the interaction with analytes having high dipole moment. Wang *et al.* synthesized *epsilon* - WO_3 nanoparticles by means of flame spray pyrolysis. Cr dopants were used to stabilize the *epsilon* _ phase [59]. Si-doped WO_3chemoresistive sensors were used to thermally stabilize the acetone selective *epsilon* - WO_3 phase at the operating temperat*ures* 300-500_C as an alternative to doping with potentially toxic Cr [27-38]. Righettoni et al. [60] developed a portable exhaled breath acetone sensor based on a back-heated substrate with a sensing film of WO_3 nanoparticles doped with Si. The sensor could detect acetone even at low concentrations up to 20 ppb. Güntner *et al.* [61] developed an WO_3:Si acetone sensor combining with a sampler that extracted and buffered the end-tidal fraction of breath. This sampler was applied for prolonged sensor exposure.

In past years, the researches were prepared most of the WO_3 sensors by methods sol-gel, electrospinning, hydrothermal and glancing angle deposition methodology. They have been used to improve acetone sensing characteristics [62–64]. The advantages and disadvantages of different techniques are summarized in Table 1 [1]. In addition to morphology control, doping and dimension control are used to improve the gas sensitivity and selectivity of WO_3. For example, Gao *et al.* [65] prepared Cr_2O3-doped WO_3 thin films by sol–gel method. The acetone sensing properties are a function of the porous structure, the Cr_2O_3 content, the sintering temperature and the cooling way. Xiao *et al.* [66] prepared Cu-doped WO_3 hollow fibers by electrospinning technique, combined with the sol–gel method.

Choi et al. [67] prepared bumpy WO_3hemitube nanostructure via O_2 plasma surface modification of electrospun fiber templates. The WO_3 hemitubes were functionalized with graphene-based material utilizing either thin graphite (GR) or graphene oxide (RGO) layers for the detection of acetone and hydrogen sulfide (H2S). The sensing properties of the GR (0.1 wt %)- WO_3 and GO (0.1 wt %)-WO3 hemitube sensors were investigated in highly humid ambient (85−95% RH) and the sensors exhibited highly H_2S as well as acetone selective characteristics with respect to various interfering biomarker gases. The superior sensing properties were ascribed to the electronic sensitization of graphene based materials by modulating space charged layers at the interfaces between n-type WO_3 hemitubes and p-type graphene-based materials. The use of graphene-based additives significantly enhanced the acetone sensing characteristics of such composite materials for exhaled breath analysis.

Better gas sensing properties of Cu-doped triclinic WO_3 hollow fibers were attributed to the high surface-to-volume ratio of WO_3 hollow fiber, junction structure, and triclinic phase composition, which strengthened the interaction between acetone and WO_3 on the surface.

Xiao *et al.* [70] synthesized C-doped WO_3 polycrystalline materials by using cotton fibers as a template and carbon source. The C-doped WO_3sensor showed good long term stability. Upadhyay et al. [71] developed a new acetone sensor based on In-doped WO_3 nanostructures. The increasing of the responses to acetone vapor was connected with the change in the surface morphology of the WO_3 upon indium doping which affects the extent of adsorption of atmospheric oxygen on the surface of sensors.

1D WO_3 nanotubes with the average diameter of about 200 nm by electrospinning were synthesized. The surface of the produced nanotubes was rough and full of protuberances which could provide more space for electrons on the surface of WO_3 to react with target gas and makes an enhancement in the sensitivity. WO_3nanofibers with a porous morphology by electrospinning method were prepared. They allowed detection of acetone down to 0.1 ppm even at 95% relative humidity. The Si-doped WO_3, WO_3nanofiber scaffold and WO_3/Pt-decorated rGO nanosheets were also applied for acetone sensing. [69-71]. Shen et al. alsosynthesized hierarchical walnut-like Fe-C-codoped WO_3microspheres for application in the breath acetone analysis. The amount of Fe doping was optimized based on detecting the acetone responses dependent on the operating temperature and exhibited high response to acetone and very low responses to NH_3, CO, toluene, methanol, ethanol and NO.

Other promising research efforts in developing highly selective and sensitive exhaled breath sensors are combining noble catalysts and unique metal oxide nanostructures [73,74]. Selective detection, high surface area and high porosity are some of several advantages of this approach. For instance,

Shin *et al.* [75] synthesized polycrystalline WO_3 fibers functionalized by catalytic Pt and IrO_2 nanoparticles to prepare chemiresistive sensors for exhaled breath analyses of diabetes and halitosis by detecting acetone and H_2S in a humid atmosphere (RH 75%). The Pt-WO_3 fibers showed a higher acetone response and also a superior response to H_2S compared to pristine WO_3 fibers. Beside, IrO_2- WO_3 fibers showed the temperature-independent sensing properties and selective response to H_2S. Thus, the highly selective cross-response between H_2S and acetone was successfully achieved via the combination of IrO_2 particles on WO_3 fibers. This group suggests the p-type semiconductor property of PtO (0.86 eV) and the n-type semiconductor property of IrO_2 (2.34 eV) resulted in totally distinct sensor properties driven by chemical sensitization and electrical sensitization, respectively. Choi *et al.* [75] synthesized thin-walled WO_3 hemitube and catalytic Pt functionalized WO_3 hemitubes via a polymeric fiber-templating route for the detection of H_2S and acetone. WO_3 hemitubes showed superior hydrogen sulfide sensing properties with minimal response to acetone and toluene at 85 RH% while Pt functionalized WO_3 hemitubes exhibited superior acetone response with negligible H_2S response. As mentioned above, small crystal size and large specific surface area are definitely advantageous to improve gas sensing response. Kim et al. [78] prepared WO_3nanofibers (NFs) functionalized by Rh_2O_3 nanoparticles (NPs) with high sensing properties toward acetone at humid atmosphere (95%). The increased oxygen vacancies in WO_3, caused by functionalization of Rh_2O3 NPs and catalytic sensitization of Rh_2O_3 NPs on WO_3 NFs were discussed as the reasons for the improved sensing properties of the fabricated

sensor. Yin *et al.* [78] developed RuO_2 NPs loaded WO_3 NFs for potential diagnosis of diabetes. Recently, studies using apoferritin as a protein template have been researched for uniform loading of catalyst NPs on supporting scaffold layers. Apoferritin is a sphere-shaped protein with the size of 12 nm consisting of 24 protein subunits. It includes a sphere-shaped inner cavity with 7–8 nm in diameter, which can encapsulate ions and metal within the hollow cage. Importantly, the outer surface of apoferrit in is positively charged, generating repulsive force between individual apoferritins to induce well dispersed apoferritins. Apoferritin as a suitable template and electrospining as an effective method for nanofiber synthesis were employed for the preparation of sensing material. The improved acetone gas response of the fabricated sensor was attributed to electronic sensitization behavior of RuO_2 and the increased oxygen vacancies generated by RuO_2.

The design and control of the surface state is another possible way to obtain good gas sensitivity and selectivity. Different crystallographic facets corresponding to different shapes of metal oxides have distinctive surface atom structures and surface energies, which have been demonstrated in the chemical reactivity and sensing property of nano- and microsized crystals. So, it is momentous to predict and control the exposed facets and investigate the facet-dependent sensing properties of metal oxides [78-80]. For instance, Jia *et al.* [77] synthesized WO_3 nanorods with exposed (100) and (002) facets via a hydrothermal approach using different directing agents and the effect of exposed facets on acetone sensing properties were investigated. It was realized that WO_3 samples with exposed (002) facets exhibited better acetone sensitivity and selectivity than those with (100) facets against ethanol and other reducing gases. They stated that the asymmetric distribution of unsaturated coordinated O atoms in the O-terminated (002) facets, leads to distortion of the electron cloud and production of local electric dipole moment on the surface. This local electric dipole moment increases the interaction with analytes having high dipole moment (e.g., acetone) which brings selectivity to WO_3nanorods with exposed (002) facets. In addition, high gas sensitivity is a consequence of the large number of oxygen vacancies and defects on the (002) facets [81]. Al-Hadeethi *et al.* [82] successfully synthesized cuboid WO_3nanosheets with exposed (020) and (200) facets by a low-temperature acid-assisted (HCl) hydrothermal process. The high acetone selectivity was related to the asymmetric arrangement of O atoms on the exposure facets, which cause the non-uniform distribution of electron cloud on the exposed facets. The high sensitivity of WO_3nanosheets to the organic vapors with high dipole moment is due to the local electric polarization on the exposed facets. Alizadeh et al. [1] II data about the optimum temperature, response and recovery times and detection limits of some developed WO_3 acetone sensors are collected in Table 1 [1].

The sensing response of pure WO_3 and C-doped WO_3sintered at different temperatures to acetone in the concentration range of 0.2–5 ppm at operating temperature 300◦C is shown in Figure 5.

ZnO Based Chemiresistors

Zinc oxide (ZnO) is an inorganic compound with a wide bandgap 3.3 eV. ZnO has attracted considerable attention because of its good response to different gases [47,80,81]. Doping with different metals such as Sn [83], Mn [83,84], Co [85], Ni [86], Cr [87], Rh [88], Al [89], rare earth metal [32], [90], CuO [91] and also utilization of noble metal such as Au [92–94] and Pt [95] led to improve response of ZnO-based acetone detectors (see Figure 6). Rare earth metals, such as La and

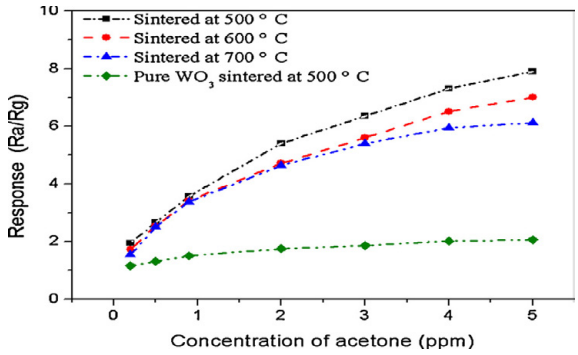

Figure 5: The sensing response of pure WO_3 and C-doped WO_3 sintered at different temperatures to acetone in the concentration range of 0.2–5 ppm at operating temperature 300°C.

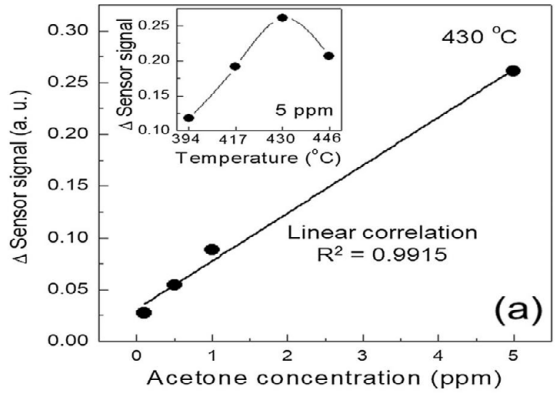

Figure 6: Highly selective real-time detection of breath acetone by using ZnO quantum dotwith a miniaturized gas chromatographic column.

Ce, due to their excellent catalytic properties, have been utilized as sensitizers because they can increase the number of active sites on the surface of semiconducting oxides.Taking into account that Au nanoparticles can activate the dissociation of molecular oxygen, the enhanced sensing properties were obtained [96]. Various ZnO quantumdots and nanocomposites have been introduced for acetone detection such as $ZnFe_2O_4$[97-99], Zn_2SnO_4[100], $ZnSnO_3$ [101], ZnO-CuO [102], SnO_2-ZnO [103-104], ZnO/$ZnCo_2O_4$ [105], ZnO/graphene [106–108], ZnO-CuO/graphene oxide [109], graphene-$ZnFe2O_4$[110] and ZnO– In_2O_3[111].

ZnO based acetone sensors have various forms, such as thin films, nanofibers, nanorods, nanowires, porous nanoparticlesetc. [91-96]. Highly selective detection of acetone in respiration was observed in a ZnO sensor with quantum dots. Improved sensing properties to acetone shown solid and hollow ZnO nanofibers [91], snowflake -like ZnO structures [43]. Various hierarchical ZnO architectures, including dumbbell-like ZnO [97], dandelon-like [98], flower-like [99,100], porous rectangular plate [101], hollow nano cage [102] and nano comb [44] have been prepared by different methods for acetone detection. The dandelion-like ZnO gas sensor to acetone exhibited remarkable selectivity for acetone in 90% of relative humidity (RH) and good selectivity towards acetone concentration of higher than 10 ppm [97]. The synthesis of stable three-dimensional (3D) hierarchically assembled porous uniform rectangular ZnO plate It was reported. Chen *et al.* proposed a hierarchical nan comb structure ZnO gas sensor for the task of acetone detection [102]. Li *et al.* synthesized hierarchical hollow ZnOnanocages which could detect acetone in ppb level with good selectivity [95].

Fe_2O_3 Based Chemiresistors

Hematite (α-Fe_2O_3) which is the most stable iron oxide under ambient conditions. The information about Fe_2O_3chemiresistors collected in [1]. Remarkable efforts have been allocated to the construction of α-Fe_2O_3 based sensors sensitive to acetone [Ma *et al.* [112], Sun *et al.* [113], Guo *et al.* [114]. The enhanced sensing properties were connected with wide porous distribution of the nanoscale Fe_2O_3, small particle size, high surface area., and formation of sufficient electron depletion area.

Successfully synthesized hollow and porous Fe_2O_3 nanotubes were realized by a single nozzle electro spinning method following with annealing process. Kim *et al.* [115] studied hematite nanotube array synthesized by anodization method. Gunawan*et al.* [116] synthesized Au-decorated 1D Fe_2O_3 acetone sensors via microwave irradiation method. The presence of Au NPs is elevated the dissociation of O_2 better in replenishing O vacancies, thereby increasing the immediate supply of lattice oxygen to the oxidation of acetone, which leads to ultra-high sensitivity towards acetone. Shan *et al.* [117] investigated the effect of La doping on the acetone sensing behavior of Fe_2O_3 nanotubes. Electro spinning followed by calcination led to enhancement in the electrical transport properties of the sensor due to the presence of La, reduction of the grain size and so enlargement in surface sites for reactions and the catalytic activity of La for the conversion of the reducing gas into the respective oxidation product.

The response of the sensor to acetone was depended on humidity and decreased by increasing the RH. Liu *et al.* [118] compared the acetone sensing properties of electrospuned pristine and Ce doped α- Fe_2O_3 nanotubes. They explained the better acetone sensitivity of Ce doped Fe_2O_3 nanotubes by the formation of more defect on the surface of Fe_2O_3 nanotube after doping Ce(IV) could lead to a larger contact area between acetone and sensing material and also the catalytic behavior of Ce for the conversion of the reducing gas into the respective oxidation product. Jin *et al.* [119] reported the synthesis and sensing characterization of monodisperse porous pure and Cu-doped Fe_2O_3microcubes, microcakes and microspheroids. The improved acetone sensing properties of Cu-doped Fe_2O_3 particles than the pure one was relevant to the increasing active sites in doped particles, large surface area, pore size, and catalytic properties of Cu. Chakraborty *et al.* [120] used sonochemically prepared nanosized Fe_2O_3 sensors to detect human breath. Biswal [121] synthesized pure and Pt-loaded nanocrystalline Fe_2O_3 by precipitation using ultrasonic irradiation. He observed 55% enhancement in response to acetone by the addition of 1wt% Pt to alfa- Fe_2O_3. 1D/2D α- Fe_2O_3/SnO_2 hybrid nanoarrays for sub-ppm acetone detection were investigated in [122]. The response on NiO, α-Fe_2O_3, and α-Fe_2O_3 / NiO samples per 100 ppm acetone at different operating temperatures is shown in Figure 7 (see [123]). Improved gas-sensitive characteristics in acetone were observed in nanowires (rods) from α-Fe_2O_3 / NiO heterojunctions[123].

The results of response measurements for a patented acetone sensor shown in Figure 8 [53], a composition for detecting acetone for it, and a method for its preparation of which is proposed. The composition includes Y-iron oxide (Y-Fe_2O_3), antimony salt and platinum (Pt) contacts. The inventors noted that a sensor made using the above formulation is selective for a low concentration of acetone for respiration. In this US patent, measurements were carried out in a very small, unsatisfactory for practice, acetone concentration is 0.75-1.25 ppm (Figure 8). Perhaps such semiconductor sensors for diabetes monitoring are non-invasive, but expensive. The measurements of the characteristics of sensors based on Y-Fe-O were carried out at an operating temperature of 300°C.

In_2O_3 Based Chemiresistors

Indium oxide (In_2O_3) is an n-type semiconductor with a wide bandgap of 3.55–3.75 eV. Their sensing performance improvement can be realized by involving of Au [124–128], Pt[129], Pd[130] on the surface of this material. Various In_2O_3 based gas sensors with different morphologies such as sphere nanoparticles [131,132], hollow nanofiber[133], porous hollow spheres [49], hierarchical nanostructure [134-144], nanowire and nanotube [124] have been developed for acetone detection. Xing *et al.* [124] fabricated the ordered three-dimensional inverse opal (3DIO) macroporous

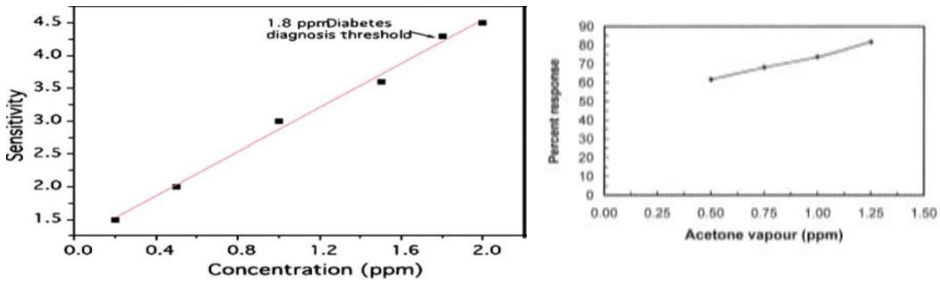

Figure 7: α-Fe_2O_3/NiO heterojunctionnanorods with enhanced gas sensing performance for acetone.

Figure 8: A type of an acetone microelectronic monitor.

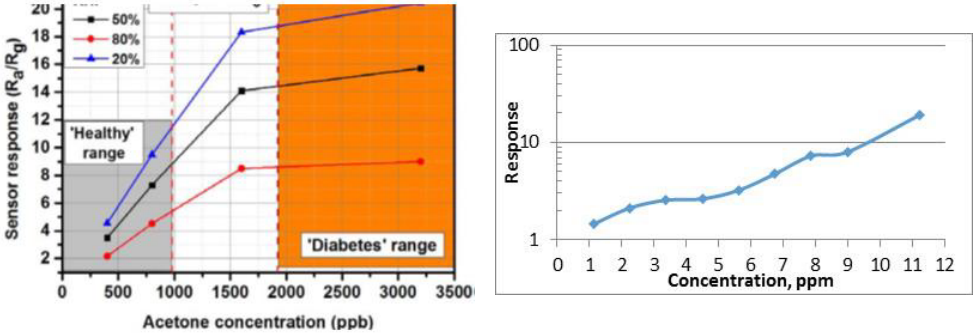

Figure 9: "Healthy" and "diabetic" regions in the sensor of silicon-doped WO_3 acetone [151].

In_2O_3 films to determine acetone detection in human breath. Theyproposed three-dimensional In_2O_3–CuO inverse opals for selective acetone detection.

TiO_2 Based Chemiresistors

Titanium dioxide (TiO_2) has the stability, low-cost, and nontoxicity. TiO_2 is usually a stable n-type material in the rutile phase. However, some reports are published on sol–gel derived undoped p-type TiO_2 thin film with anatase phase. The non-stoichiometric p-type TiO_2 originates either from Ti vacancy or from oxygen interstitials [145]. Rell *et al.* [146] developed a new technique for the deposition of TiO_2nanoparticle thin films - matrix-assisted pulsed laser evaporation for gas sensor manufacture. The proposed technology allowed to detect both vapors of acetone and ethanol at low concentrations (20–200 ppm in dry air). Deng *et al.* [147] realized a TiO_2nanoporous thin film based gas sensors and detected 1.5 ppm acetone under the interference of water vapor. Ding *et al.* [148] fabricated a microsized room temperature acetone sensor on photoinduced SWNT−TiO_2 nanohybrid with core/shell structure using screen printing of the commercial P25 TiO_2 paste. Such chemiresistor showed linear, fast and reversible responses to acetone at ppm-level. The screen-printed titanium dioxide (TiO_2) sensor showed sensitivity for type 1 diabetes diagnosis.

Teleki *et al.* [149] produced nanostructured anatase TiO_2 by flame spray pyrolysis and tested for sensing to of volatile acetone at 500ºC. Yang *et al.* [150] synthesized novel anatase TiO_2 hierarchical microspheres with selectively etched high-energy (001) crystal facets by a facile hydrothermal method and detected a much higher acetone response than that of TiO_2 microspheres with intact (001) facets and slightly-etched (001) facets. They proposed that (001) facets could act as active sites for gas absorption and facilitate the gas sensing reaction.

Acetone detectors made from chemisistors based on oxides of other metals are discussed in the literature. Note that there are other metal oxide-based chemi-resistive exhaled air sensors for potential use in the diagnosis of diabetes mellitus using acetone as a biomarker. Sensors with a sufficiently high response (S=Ra/Rg) to acetone have also been implemented on the following nanostructures: Fe_2O_3 / Al - ZnOnanocomposites, SnO_2 / Au-In_2O_3 core-shell nanofibers, SnO_2-Sm_2O_3 hierarchical structures, ruthenium-doped NiO balls in the shape of a flower, NiO spheres doped with W, Sm_2O_3/SnO_2, TiO_2 nanoparticles on In_2O_3nanocrystals.

Note that the choice of chemiresistive acetone sensors based on metal oxide materials (including nanostructures) is already very large. Which of these sensors will be used in real devices depends on their many parameters and, of course, on the cost of nanostructures.

Non-invasive diagnosis of deceases

Diabetes mellitus belongs to the global medical and social problems of the XXI century, which have affected the entire world community. According to the World Health Organization, the number of registered diabetes patients in the world is about 450 million peoples. Diabetes mellitus (DM) is a syndrome of impaired carbohydrate, fat, and protein metabolism caused by either lack of insulin secretion or decreased the sensitivity of the tissues to insulin. Relating this it is categorized as type I diabetes (It is called insulin-dependent diabetes mellitus (IDDM) and is caused by lack of insulin secretion) and type II diabetes (It is called non–insulin-dependent diabetes mellitus (NIDDM) and is caused by decreased sensitivity oftarget tissues to the metabolic effect of insulin). This reducedsensitivity to insulin is often called insulin resistance. In both types of diabetes mellitus, metabolism of all the main foodstuffs is altered.

When analyzing the effects of acetone on diabetic patients, it would probably make sense to start from the concentration of acetone 1 ppm. Most diabetics are at a relatively early stage of the disease (the concentration of released acetone is up to 10-12 ppm), basically they are not under the daily supervision of doctors. A miniature and easy transportable glucose (sugar) meter is needed for such patients. The dependence of the response of the gas sensor on the concentration of acetone for a healthy and sick person is shown in Figure 9 [151].

The analysis of the acetone influence for diabetic subjects has the sense to make starting 1 ppm. A type of an acetone microelectronic monitor is shown in Figure 8. For its implementation, it is necessary to have, for example, such a metal oxide sensor with a high sensitivity to acetone of the type as measured by Dr. A. Sayunts at YSU in the concentration range of 1-12 ppm on our sensor made of SnO_2<MWCNT> (see Figure 9).

We proposed early semiconductor monitors, including those using Arduino Nano processors [152-154]. Note that for the implementation of a non-invasive monitor of acetone with a tube, such as shown in Figure. 8, it is additionally necessary to develop the latter with a special mouthpiece or another device that dries out the patient's exhaled air. High humidity of exhaled air created often corresponding higher requirements to sensors. Therefore, it is necessary to develop a pre-concentrator to its. The pre-concentration technique is well known in chromatography where the separation column is filled with adsorbent molecules. The same mechanism is mostly applied for pre-concentrators to exhaled biomarkers. Two-step pre-concentration in order to reduce the humidity level in exhaled samples is preferable today.

CONCLUSION

Recently, interest has increased in semiconductor gas sensors for non-invasive control of various human diseases. The paper presents and discusses the work carried out on non-invasive metal oxide sensors (chemiresistors) for acetone exhaled by a diabetic both at Yerevan State University and abroad. Such sensors are manufactured using the methods of modern microelectronic technology. They have a low cost and high sensitivity to gas. The technologies and parameters of chemiresistors based on tin dioxide, tungsten trioxide, zinc oxide, Fe_2O_3, In_2O_3, and TiO_2 developed at YSU and in the world are presented. When analyzing the effects of acetone on diabetic patients, it is most likely to start with an acetone concentration of 1 ppm. At YSU, the response of chemiresistors made of SnO_2 doped with MWCNT was measured at a concentration of acetone released from 1 to 12 ppm, typical for diabetics at a relatively early stage of the disease. Microelectronic glucose (sugar) meter is needed.

REFERENCES

1. Alizadeh N, Jamalabadi H and Tavoli F. Breath Acetone Sensors as Non-Invasive Health Monitoring Systems IEEE Sensors J. 2020;20:5-31.
2. Aroutiounian VM. Microelectronic gas sensors for non-invasive analysis of exhaled gases. J Nanomed Nanotechnol. 2020;11:1-7.
3. Aroutiounian VM. Metal oxide gas biomarkers of diseases for medical and health applications. Biomed J Sci & Tech Res. 2020;29:22328-22336.
4. Rydosz A. A negative correlation between blood glucose and acetone measured in healthy and type-1 diabetes mellitus patient breath. J Diabetes Sci Technol. 2015;9: 881–884.
5. Chang J E, Lee D S, Ban S W, Oh J, Jung MY et al. Analysis of volatile organic compounds in exhaled human breath for lung cancer diagnosis using a sensor system. Sens Actuators. 2018;B255:800–807.
6. Herman-Saffar O, Boger Z, Libson S, Lieberman D, Gonen R et al. Early non-invasive detection of breast cancer using exhaled breath and urine analysis. Comput Biol Med. 2018;96:227–232.
7. Hanania N A, Massanari M, Jain N. Measurement of fractional exhaled nitric oxide in real-world clinical practice alters asthma treatment decisions. Ann Allergy Asthma Immunol. 2018;120:414–418.
8. Karyakin A A, Nikulina SV, Vokhmyanina A W, Karyakina DV, Anaev E E et al. Non-invasive monitoring of diabetes through analysis of the exhaled breath condensate (aerosol). Electrochem. Commun. 2017;83:81–84.
9. Liu W, Xu L, Shenget KA. Review on Graphene-based Nanocomposites for Electrochemical and Fluorescent Biosensors. NPG Asia Mater. 2018;10:293-308.
10. Aroutiounian VM. Hydrogen sensors In Dekker Encyclopedia of Nano-science and Nanotechnology, S.E. Lyshevski (Ed.). Second Edition, Taylor and Francis: New York, 2012.
11. Aroutiounian VM. Porous silicon gas sensors In: Semiconductor gas sensors (R. Jaanisco, O.K. Tan (Eds.).).Woodhead, Series in Electronic and Optical Materials, 2013; 12: 408-430.
12. Banika F.-G. Chemical and Biological sensors. Technosphera Press, 2014.
13. Aroutiounian VM .Decrease in operation temperature of zinc oxide nanomarkers. Biomedical J Sci &Techn Res. 2020; 30:23211- 23217.
14. AroutiounianVM. Properties of hydrogen peroxide sensors made from nanocrystalline materials. Sens. Transducers. 2018:; 23:9-21.
15. Aroutiounian VM. Semiconductor gas sensors for detection of chemical warfare agents and toxic industrial chemicals. Intnl Sci J Alternative Energy and Ecology. 2018;249-251:38-46.
16. Aroutiounian VM. Semiconductor gas sensors made from metal oxides functionalized with carbon nanotubes. Sensors & Transducers. 2018;228:1-16.
17. Aroutiounian VM. Graphene- and graphene-oxide-based gas sensors In: Graphene Science Handbook. Applications and Industrialization. CRC Press Tailor & Francis Group. 2016;20:299-310.
18. Aroutiounian VM. Metal oxide photoelectrodes for hydrogen generation using solar radiation-driven water splitting. Solar Energy. 2005;78:581-592.
19. Masikini M, Chowdhury M, Nemraou O. Application in Exhaled Breath Acetone Chemiresistive Sensors. J Electrochemical Society. 2020;167:037537.
20. Diabetes mellitus: diagnosis, treatment, prevention (Ed. By II Dedov, MV Shestakova). M .: LLC "Publishing House" Medical Information Agency ", 2011 (in Russian).
21. Saasa V, Malwela Th, Beukes M, Mokgotho M, Liu Ch P et al. Sensing Technologies for Detection of Acetone in Human Breath for Diabetes Diagnosis and Monitoring Diagnostics. 2018;8:12-29.
22. Ta L, Chang Sh, Chen Ch J, Liu J T. Non-Invasive Blood Glucose Monitoring Technology. Sensors 2020;0:6925-6957.
23. Ahmadnia-Feyzabad S, Khodadadi AA, Vesali-Naseh M, Mortazavi Y. Highly sensitive and selective sensors to volatile organic compounds using MWCNTs/SnO2. Sens. Actuators. 2012;B166:150-155.
24. Salehi S, Nikan E, Khodadadi AA, Mortazavi Y. Highly sensitive carbon nanotubes-SnO2 nanocomposite sensor for acetone detection in diabetes mellitus breathe. Sens Actuators. 2014;B 205:261–267.
25. Choi S J, Jang B H, Lee S J, Min BK, Rothschild A et al. Catalyst-loaded porous WO3 nanofibers using catalyst decorated polystyrene colloid templates for detection of biomarker molecules. Chem Com. 2012;3:1-14.
26. Choi S J, Fuchs F, Demadrille R, Grevin B, Jang B H et al. Macromolecular Mater Eng. 2017;302. Art. no. 1600569.
27. Xiao T, Wang XY, Zhao Z H, Li L, Zhang L. Highly sensitive and selective acetone sensor based on C-doped WO3 for potential diagnosis of diabetes mellitus. Sens Actuators. 2014;B199:210-219.
28. S.-J. Choi Selective Diagnosis of Diabetes Using Pt-Functionalized WO3 Hemitube Networks As a Sensing Layer of Acetone in Exhaled Breath. Anal Chem. 2013;85: 1792-1799.
29. Bai X, Ji H, Gao P, Zhang Y, Sun X. Morphology, phase structure and acetone sensitive properties of copper-doped tungsten oxide sensors. Sens Actuators. 2014; B193:100-106.
30. Gao P, Ji H, Zhou Y, Li X. Selective acetone gas sensors using porous WO3–Cr2O3 thin films prepared by sol-gel method. Thin Solid Films. 2012;520:3100–3106.
31. Kim KH, Kim SJ, Cho HJ, Kim NH, Jang J et al. Nanofibers functionalized by protein-templated RuO2 nanoparticles as highly sensitive exhaled breath gas sensing layers. Sens Actuators. 2017;B24:1276 -1283.
32. Kulandaisamy A J, Elavalagan V, Shankar P, Mani GK, Babu KJ. Nanostructured cerium-doped ZnO thin film-A breath sensor. Ceramics Int 2016;42:18289–18295.
33. Aroutiounian V. Metal oxide hdrogen, oxygen, and carbon monoxide sensors for hydrogen setups and cells. Intern J Hydrogen Energy 2007;32:1145-1158.
34. Zhang Z, Zhu L, Wen Z, Ye Z. Controllable synthesis of Co3O4

crossed nanosheet arrays toward an acetone gas sensor. Sens Actuators. 2017;B238:1052–1059.

35. Hu L, Li Y. Improved acetone sensing properties of flat sensors based on Co-SnO2 composite nanofibers. Environmental Science and Technology 2011;56:2644 -2648.

36. Yamazoe N. New approaches for improving semiconductor gas sensors. Sens Actuators. 1991; B: 157-158.

37. Phani AR, Manorama SV, Rao VJ. X-ray photoelectron spectroscopy studies on Pd doped SnO2 liquid petroleum gas sensor. Appl Phys Lett. 1997;71: 2358-2360.

38. Chen Y, Qin H, Cao Y, Zhao H and Hu J et al. Acetone Sensing Properties and Mechanism of SnO2 Thick-Films Sensors. 2018;18:3425-3432.

39. Patil D, Patil D , Patil P, Patil SB, Patil PP. Highly sensitive and selective LPG sensor based on -Fe2O3 nanorods. Sensors Actuators B. 2011;152:299–306.

40. Gouma P, Kalyanasundaram K, Yun X, Stanaćević M, Wang . Nanosensor and breath analyzer for ammonia detection in exhaled human breath. IEEE Sensors. 2010;10:49-53.

41. Bagal LK, Patil JY, Bagal KN, Mullaand IS, Suryavanshi SS. Acetone vapour sensing characteristics of undoped and Zn, Ce doped SnO2 thick film gas sensor. Materials Research Innovations. 2013;17:98-105.

42. Zhang Y. Light-Controlled Swarming and Assembly of Colloidal Particles. J Colloid Interface Sci. 2018;531:74-81.

43. Aroutiounian VM. Gas nanosensors made from semiconductor metal oxides. J. Contemp. Physics (Armenian Academy of Sciences 2019;54:356-367.

44. Aroutiounian VM. Acetone sensor made of tin dioxide. J. Contemp. Physics (Armenian Academy of Sciences) 2020;55:213–224.

45. Choi SJ, Jang BH, Lee SJ, Min BK, Rothschild A. Mesoporous SnO2 Nanotubes via Electrospinning–Etching Route: Highly Sensitive and Selective Detection of H2S Molecule. ACS Appl Mater Interfaces 2017:9:26304–26313.

46. Usman F, Dennis J, Meriaudeau F. Development of a surface plasmon resonance acetone sensor for noninvasive screening and monitoring of diabetes. Proc. IOP Conf. Series. Mater Sci Eng. 2018:383: Art. no. 012024.

47. Lin T, Lv X, Hu Zh, Xu A and Feng C et al. Semiconductor Metal Oxides as Chemoresistive Sensors for Detecting Volatile Organic Compounds Sensors 2019;19:233-232.

48. Jeong YJ, Koo WT, Jang JS, Kim DH, Kim MH. Nanoscale PtO2 catalysts-loaded SnO2 multichannel nanofibers toward highly sensitive acetone sensor. ACS Appl Mater Inter. 2018;10: 2016–2025.

49. Jeong YJ, Koo WT, Jang JS, Kim DH, Cho HJ. Chitosan-templated Ptnanocatalyst loaded mesoporous SnO2 nanofibers: A superior chemiresistor toward acetone molecules. Nanoscale. 2018:10:3713–13721.

50. Koo WT, Jang JS, Choi SJ, Cho HJ, Kim ID. ACS Enhanced acetone sensing properties of Pt-decorated Al-doped ZnO nanoparticles. Sens Actuators. 2019;B280: 109–119.

51. Mirzaei A, Hashemi B, Janghorban K. α-Fe2O3 based nanomaterials as gas sensors. J Mater Sci Mater Electron. 2016;27:3109–3144.

52. Jiang Z. Highly sensitive acetone sensor based on Eu-doped SnO2 electro spun nanofibers. Ceram Int. 2016;42:15881-15888.

53. Patents US. 9.470,675 B2 и EP2845009B1. Sensor composition for acetone detection in breath

54. Aroutiounian V M. Metal oxide gas sensors decorated with carbon nanotubes. Lithuanian Journal of Physics. 2015;55:319-329.

55. Aroutiounian V, Adamyan Z, Sayunts A, Khachaturyan E, Adamyan A. Comparative study of VOC sensors based on ruthenate MWCNT/SnO2 nanocomposites. Int Emerging Trends Sci Technology. 2014;1:1309-1319.

56. Ghosh R, Pin KJ, Reddy VS, Sayathilaka W, Ji D et al. Micro/nanofiber-based noninvasive devices for health monitoring diagnosis and rehabilitation. Applied Physics Reviews. 2020;7:041309.

57. Narjinary M, Rana P, Sen A, Pal M. Enhanced and selective acetone sensing properties of SnO2-MWCNT nanocomposites: Promising materials for diabetes sensor. Mater Des. 2017;115:158–164.

58. Wang L, Teleki A, Pratsinis SE, Gouma PI. Ferroelectric WO3 nanoparticles for acetone selective detection. Chem Mater. 2008;20:4794–4796.

59. Staerz A, Weimar U, Barsan N. Understanding the potential of WO3 based sensors for breath analysis. Sensors. 2016;16:1815-1830.

60. Righettoni M, Tricoli A, Pratsinis SE. Si: WO3 sensors for highly selective detection of acetone for easy diagnosis of diabetes by breathe analysis. Anal Chem. 2010;82: 3581–3587.

61. Güntner A, Noriane T, Sievi A, Theodore S, Gulich T. Non-invasive body fat burn monitoring from exhaled acetone with Si-doped WO3 sensing nanoparticles. ACS Sensors. 2019;4:268-287.

62. Rydosz A, Szkudlarek A, Ziabka M, Domanski K, Maziarz W. Performance of Si-doped WO3 thin films for acetone sensing prepared by glancing angle DC magnetron sputtering. IEEE Sensors J. 2016;16:1004–1012.

63. Teoh W Y, Amal R, Mädler L. Flame spray pyrolysis: An enabling technology for nanoparticles design and fabrication. Nanoscale. 2010;2:1324–1347.

64. Solero G Nanosci. Nanotechnol Synthesis of nanoparticles through flame spray pyrolysis: Experimental apparatus and preliminary results. Nanosci Nanotechnol. 2011;7:21–25.

65. Gao P, Ji H, Zhou Y, Li X. Hydrothermal synthesis of ZnO structures formed by high-aspect-ratio nanowires for acetone detection. Thin Solid Films. 2012;520:3100 -3109.

66. Xiao T. Highly sensitive and selective acetone sensor based on C-doped WO3 for potential diagnosis of diabetes mellitus. Sens Actuators. 2014:B199:210–219.

67. Upadhyay SB, Mishra RK, Sahay PP. Enhanced acetone response in co-precipitated WO3 nanostructures upon indium doping. Ibid. 2015;B209:368–376.

68. Chen L. Fully gravure-printed WO3/Pt-decorated rGO nanosheets composite film for detection of acetone. Ibid. 2018;B255:1482–1490.

69. Güntner AT. Sniffing entrapped humans with sensor arrays. Anal Chem. 2018:90, 4940–4945.

70. Kim D H, Jang J S, Koo W T, Choi S J and Kim S J et al.Hierarchically interconnected porosity control of catalyst-loaded WO3 nanofiber scaffold: Superior acetone sensing layers for exhaled breath analysis. Sens. Actuators 2018; 259:616–625.

71. Wang D, Zhang Q, Hossain M R and Johnson M. High sensitive breath sensor based on nanostructured K2W7O22 for detection of type 1 diabetes.IEEE Sensors J. 2018;18:4399–4404.

72. Shen J Y. Iron and carbon codoped WO3 with hierarchical walnut-like microstructure for highly sensitive and selective acetone sensor. Sens Actuators. 2018:B256: 27–37.

73. Da Silva L F. Acetone gas sensor based on α-Ag2WO4 nanorods obtained via a microwave-assisted hydrothermal route. J Alloys Compounds. 2016;683:186–190.

74. Chen L. Fully gravure-printed WO3/Pt-decorated rGO nanosheets

composite film for detection of acetone. Sens Actuators. 2018:B255:1482–1490.

75. Shin J, Choi S J, Youn DY and Kim I D. Exhaled VOCs sensing properties of WO3 nanofibers functionalized by Pt and IrO2 nanoparticles for diagnosis of diabetes and halitosis. J Electroceram 2012:29:106–116.

76. Abdullah Q N, Yam F K, Hassan Z andBououdina M. Pt-decorated GaN nanowires with significant improvement in H2 gassensing performance at room temperature. J Colloid Interface Sci. 2015;460:135–145.

77. Jia QQ, Ji HM, Wang DH, Bai X, Sun XH. Exposed facets induced enhanced acetone selective sensing property of nanostructured tungsten oxide. J Mater Chem A. 2014;2:13602–13611.

78. Yin M, Yu L, Liu S. Synthesis of thickness-controlled cuboid WO3 nanosheets and their exposed facets-dependent acetone sensing properties. J Alloys Compounds. 2017;696: 490–497.

79. Arya S K, Saha S, Ramirez-Vick J E, Gupta V, Bhansali S. Recent advances in ZnO nanostructures and thin films for biosensor applications: Review. Analytica Chim Acta. 2012;737:1–21.

80. Spencer M J S. Gas sensing applications of 1D-nanostructured zinc oxide: Insights from density functional theory calculations. Progr Mater Sci. 2012;57:437–486.

81. Kołodziejczak-Radzimska A, Jesionowski T. Zinc oxide—From synthesis to application: A review. Materials. 2014;7:2833–2881.

82. Al-Hadeethi Y. 2D Sn-doped ZnO ultrathin nanosheet networks for enhanced acetone gas sensing application. Ceram Int. 2017;43:2418–2423.

83. Darvishnejad MH, Firooz AA, Beheshtian J, Khodadadi A. A Highly sensitive and selective ethanol and acetone gas sensors by adding some dopants (Mn, Fe, Co, Ni) onto hexagonal ZnO plates. RSC Adv. 2016;6:7838–7845.

84. Wang J. Highly sensitive and selective ethanol and acetone gas sensors based on modified ZnO nanomaterials. Mater Des. 2017:121:69–76.

85. Liu L. Improved selective acetone sensing properties of Co-doped ZnOnanofibers by electrospinning. Sens. Actuators B Chem. 2011;155:782–788.

86. Zhang X, Dong Z, Liu S, Shi Y and Dong Y et al. Maize straw-templated hierarchical porous ZnO: Ni with enhanced acetone gas sensing properties. Sens. Actuators 2017: B 243:1224–1230.

87. Zhang G H. Morphology controlled syntheses of Cr doped ZnO single-crystal nanorods for acetone gas sensor. Mater. Lett. 2016:165:83–86.

88. Chen Z, Lin Z, Hong Y, Li N andXu M. Hydrothermal synthesis of hierarchically porous Rh-doped ZnO and its high gas sensing performance to acetone. J. Mater. Sci., Mater. Electron. 20162:7:2633–2639.

89. Koo A, Yoo R, Woo S P, Lee H S and Lee W. Enhanced acetone sensing properties of pt-decorated al-doped ZnO nanoparticles. Sens. Actuators 2019:B280:109–119.

90. Xie Y, Xing R, Li Q, Xu L and Song H. Three-dimensional ordered ZnO–CuO inverse opals toward low concentration acetone detection for exhaled breath sensing. Sens. Actuators 2015:B211:255–262.

91. Li Y, Lv T, Zhao F X, Lian X X andZou Y L et al. Enhanced acetone-sensing performance of Au/ZnO hybrids synthesized using a solution combustion method. Electron. Mater. Lett., 2015:11:890–895.

92. Lin Y. Highly stabilized and rapid sensing acetone sensor based on Au nanoparticle-decorated flower-like ZnO microstructures. J. Alloys Compounds 2015:650:37–44.

93. Meng F. Sub-ppb detection of acetone using Au-modified flower-like hierarchical ZnO structures Sens. Actuators 2015:B219:209–217.

94. Zhou X. Highly sensitive acetone gas sensor based on porous ZnFe2O4 nanospheres. Sens. Actuators 2015:B206:577–583.

95. Li X. Double-shell architectures of ZnFe2O4 nanosheets on ZnO hollow spheres for high-performance gas sensors. ACS Appl. Mater. Inter. 2015:7:17811–17818.

96. Zhou X. Nanosheet-assembled ZnFe2O4 hollow microspheres for high-sensitive acetone sensor. ACS Appl. Mater. Inter. 2015:7:15414–15421.

97. Wang Y. Mesoporous ZnFe2O4 prepared through hard template and its acetone sensing properties. Mater. Lett. 2016:183:378–381.

98. Jung H. Highly selective real-time detection of breath acetone by using ZnO quantum dots with a miniaturized gas chromatographic column. Sens. Actuators 2018:B274: 527–532.

99. Zhang Z, Zhang T, Zhou T, Lou Z and Deng J et al. Fast and real-time acetone gas sensor using hybrid ZnFe2O4/ZnO hollow spheres. RSC Adv. 2016:6: 66738–66744.

100. Yang H M. Self-assembly of Zn2SnO4 hollow microcubes and enhanced gas-sensing performances. Mater. Lett. 2016:182:264–268.

101. Chen Q. Synthesis of novel ZnSnO3 hollow polyhedrons with open nanoholes: Enhanced acetone-sensing performance. Ceram. Int. 2017:43:1617–1621.

102. Yan S H. Preparation of SnO2–ZnO hetero-nanofibers and their application in acetone sensing performance. Mater. Lett. 2015:159:447–450.

103. Choi H J, Choi S J, Choo S, Kim I D and Lee H et al. Hierarchical ZnO Nanowires-loaded Sb-doped SnO2-ZnO micrograting pattern via direct imprinting-assisted hydrothermal growth and its selective detection of acetone molecules. Sci. Rep. 2016:6: Art no. 18731.

104. Koo W T, Choi S J, Jang J S and Kim I D. Metal-organic framework templated synthesis of ultrasmall catalyst loaded ZnO/ZnCo2O4 hollow spheres for enhanced gas sensing properties. Ibid 2017:7:Art. no. 45074.

105. Wang P. ZnO nanosheets/graphene oxide nanocomposites for highly effective acetone vapor detection. Sens. Actuators 2016:B230:477–484.

106. Vessalli B A, Zito C A, Perfecto T M, Volanti D P and Mazon T. ZnOnanorods/graphene oxide sheets prepared by chemical bath deposition for volatile organic compounds detection. J. Alloys Compounds 2017:696:996–1003.

107. Zhang H, Cen Y, Du Y and Ruan S. Enhanced acetone sensing characteristics of ZnO/Graphene composites. Sensors 2016:16:1876-1884.

108. Wang C. Reduced graphene oxide decorated with CuO–ZnO hetero-junctions: Towards high selective gas-sensing property to acetone. J. Mater. Chem. A 2014:2:18635–18643.

109. Liu F, Chu X, Dong Y, Zhang W and Sun W et al. Acetone gas sensors based on graphene-ZnFe2O4 composite prepared by solvothermal method. Sens. Actuators 2013:B188:469–474.

110. Chi X. Synthesis of pristine In2O3/ZnO–In2O3 composited nanotubes and investigate the enhancement of their acetone sensing properties Mater. Sci. Semicond. Process. 2014: 27:494–499.

111. Ma J. Porous platelike hematite mesocrystals: Synthesis, catalytic and gas-sensing applications. J. Mater. Chem. 2012:22:11694–11700.

112. Sun X, Ji H, Li X, Cai S, Zheng C. Open-system nanocasting synthesis of nanoscaleα-Fe2O3 porous structure with enhanced acetone-sensing properties. J Alloys Compounds. 2014:600:111–117.

113. Guo X, Zhang J, Ni M, Liu L and Lian H et al. Comparison of gas sensing properties based on hollow and porous α-Fe2O3 nanotubes. J Mater Sci Mater Electron. 2016;27:11262–11267.

114. Kim D H. Vertically ordered hematite nanotube array as an ultrasensitive and rapid response acetone sensor. ACS Appl Mater Inter. 2014;6:14779–14784.

115. Gunawan P. Ultrahigh sensitivity of Au/1D α-Fe2O3 to acetone and the sensing mechanism. Langmuir 2012:28:14090–14099.

116. Shan H. Highly sensitive acetone sensors based on La-doped α-Fe2O3 nanotubes. Sens. Actuators 2013:B184:243–247.

117. Liu C, Shan H, Liu L, Li S and Li H. High sensing properties of Ce-doped α-Fe2O3 nanotubes to acetone. Ceram. Int. 2014:40:2395–2399.

118. Lin W X. Hydrothermal synthesis of monodisperse porous cube, cake and spheroid-like α-Fe2O3 particles and their high gas sensing properties. Sens. Actuators 2015:B220: 243–254.

119. Chakraborty S, Banerjee D, Ray I andSen A. Detection of biomarker in breath: A step towards noninvasive diabetes monitoring. Current Sci.2008:94:237–242.

120. Biswal R C. Ibid Pure and Pt-loaded gamma iron oxide as sensor for detection of sub ppm level of acetone. Sens. Actuators 2011:B157:183–188.

121. Jo Y M, Lim K, Choi H J, Yoon J W and Kim S Y et al. 2D metal-organic framework derived co-loading of Co3O4 and PdO nanocatalysts on In2O3 hollow spheres for tailored design of high-performance breath acetone sensors. Sens Actuators 2020:B325:128821.

122. Sorocki J,Rydosz A ,Staszek KG, Zhao Ch andNiu G et al. Wideband microwave multiport-based system for low gas concentration sensing and its application for acetone detection. Ibid 2020:B323:2196063.

123. AleksanyanMC, SayntsA G, Aroutiounian V M, Shahnazaryan GE and Shashkhatuni GH et al. The effect of UV irradiation on the sensitivity of acetone vapours sensor. J. Cont. Phys. - Armenian Academy of Sciences 2021:56.

124. Xing R. Au-modified three-dimensional In2O3 inverse opals: Synthesis and improved performance for acetone sensing toward diagnosis of diabetes. Nanoscale 2015:7:13051–13060.

125. Xing R. Preparation and gas sensing properties of In2O3/Au nanorods for detection of volatile organic compounds in exhaled breath. Sci. Rep. 2015:5: Art no. 10717.

126. Zhang S. Highly sensitive detection of acetone using mesoporous In2O3 nanospheres decorated with Au nanoparticles. Sens. Actuators 2017:B242:983–993.

127. Li F, Zhang T, Gao X, Wang R and Li B. Coaxial electrospinning heterojunction SnO2/Au-doped In2O3 core-shell nanofibers for acetone gas sensor. Sens. Actuators 2017:B252: 822–830.

128. Karmaoui M. Pt-decorated In2O3 nanoparticles and their ability as a highly sensitive sensor Ibid 2016:B230:697–705.

129. Gong F. 3D hierarchical In2O3 nanoarchitectures consisting of nano cuboids and nanosheets for chemical sensors with enhanced performances. Mater. Lett. 2016:163,236–239.

130. Liu H, Qu F, Gong H, Jiang H and Yang M,et al. Template-free synthesis of In2O3 nanoparticles and their acetone sensing properties. Mater. Lett. 2016:182:343010–343016.

131. Wang S. Facile fabrication and enhanced gas sensing properties of In2O3 nanoparticles. J. Chem. 2014:38:4879–4884.

132. Liang X. Synthesis of In2O3 hollow nanofibers and their application in highly sensitive detection of acetone. Ceram. Int. 2015:41:13780–13787.

133. Wang S, Cao J, Cui W, Li X and Li D et al. Facile synthesis and high acetone gas sensing performances of popcorn-like In2O3 hierarchical nanostructures. Mater. Lett. 2017:186: 256–258.

134. Liu L, Li S, Guo X, Wang L and Liu L et al. The fabrication of In2O3 nanowire and nanotube by single nozzle electrospinning and their gas sensing property. J. Mater. Sci., Mater. Electron. 2016:27:5153–5157.

135. Xing R, Sheng K, Xu L, Liu W and Song J et al. Three dimensional In2O3–CuO inverse opals: Synthesis and improved gas sensing properties towards acetone. RSC Adv. 2016: 6:57389–57395.

136. Park S. Acetone gas detection using TiO2 nanoparticles functionalized In2O3 nanowires for diagnosis of diabetes. J. Alloys Compounds 2017:696:655–662.

137. Chen C, Li J, Mi R and Liu Y. Enhanced gas-sensing performance of one-pot-synthesized Pt/CdIn2O4 composites with controlled morphologies. Anal. Methods 2015:7:1085–1091.

138. Anand K, Kaur J, Singh R C and Thangaraj R. Temperature dependent selectivity towards ethanol and acetone of Dy3+-doped In2O3 nanoparticles. Chem. Phys. Lett. 2017:670: 37–45.

139. Bai J and Zhou B. Titanium dioxide nanomaterials for sensor applications. Chem. Rev. 2014:114:10131–10176.

140. Yang Y, Liang Y, Hu R, Yuan Q and Zou Z et al. Anatase TiO2 hierarchical microspheres with selectively etched high-energy {001} crystal facets for high-performance acetone sensing and methyl orange degradation. Mater. Res. Bull. 2017: 94:272–278.

141. Guo W, Feng Q, Tao Y, Zheng L and Han Z et al. Systematic investigation on the gas-sensing performance of TiO2 nanoplate sensors for enhanced detection on toxic gases. Mater. Res. Bull. 2016:73:302–307.

142. Wang Y A. High-response ethanol gas sensor based on one dimensional TiO2/V2O5 branched nano heterostructures. Nanotechnology. 2016:27: Art. no. 425503.

143. Wang Y, Wang S, Zhang H, Gao X and Yang J et al. Brookite TiO2 decorated α-Fe2O3 nano heterostructures with rod morphologies for gas sensor application. J. Mater. Chem. A 2014:2:7935–7943.

144. Hazra A. Influence of temperature, voltage and hydrogen on the reversible transition of electrical conductivity in sol–gel grown nanocrystalline TiO2 thin film. J. Mater. Sci., Mater. Electron. 2013:24:1658–1663.

145. Hossein-Babaei F, Keshmiri M, Kakavand M andTroczynski T A. Resistive gas sensor based on undoped p-type anatase. Sens. Actuators 2005:B110:28–35.

146. Rella R. Acetone and ethanol solid-state gas sensors based on TiO2 nanoparticles thin film deposited by matrix assisted pulsed laser evaporation. Ibid 2007:127:426.

147. Deng L L, Zhao C X, Ma Y, Chen S S and Xu G et al. Low cost acetone sensors with selectivity over water vapor based on screen printed TiO2 nanoparticles. Anal. Methods 2013:5: 3709.

148. Ding M, Sorescu D C and Star A. Photoinduced charge transfer and acetone sensitivity of single-walled carbon nanotube–titanium dioxide hybrids. J. Amer. Chem. Soc 2013:135: 9015–9022.

149. Teleki A, Pratsinis SE, Kalyanasundaram K and Gouma P I. Sensing of organic vapours by flame-made TiO2 nanoparticles. Sens. Actuators 2006:B119:683–690.

150. Rydosz A. Sensors for enhanced detection of acetone as a potential tool for non-invasive diabetes monitoring. Sensors 2018:18:2298-2312.

151. Aroutiounian VM and Hovhannisyan A. Breath Semiconductor Metal Oxide Gas Detector using Arduino Nano Biomed J Sci & Tech Res. 27, 20422 -24(2020).

152. Aroutiounian VM and Hovhannisian A. Semiconductor gas sensors detector using Arduino NANO. Ibid. 2019;12:283-287.

153. Aroutiounian V and Kirakosyan V. Flexible gas detector. J Arm J Physics. 2018;11:160-165.

154. Aroutiounian V, Pokhsraryan D and Chilingaryan H. Gas monitoring system. Ibid. 2010;3:78-81.